

On the Thermodynamic Stability of BiFeO₃

Sverre M. Selbach, Mari-Ann Einarsrud, and Tor Grande*

Department of Materials Science and Engineering, Norwegian University of Science and Technology,
7491 Trondheim, Norway

Received September 29, 2008. Revised Manuscript Received November 7, 2008

The thermodynamic stability of BiFeO₃ is investigated by high temperature X-ray diffraction and isothermal heat treatment of Bi₂O₃–Fe₂O₃ powder mixture as well as phase pure BiFeO₃ prepared by a wet chemical route. Experimental evidence for decomposition of BiFeO₃ to Bi₂₅FeO₃₉ and Bi₂Fe₄O₉ in the temperature interval 720–1040 K is reported. The experimental observations are discussed in terms of available thermodynamic data for the system. Finally, the stability of BiFeO₃ and related Bi-based perovskites is discussed in relation to Goldschmidt tolerance factor and the influence of pressure and chemical substitution.

Introduction

The perovskite BiFeO₃ has received rapidly increasing attention since the first report of enhanced multiferroic¹ properties in epitaxial thin films.² BiFeO₃ belongs to the rhombohedral space group *R3c* and was recently shown to transform to the orthorhombic space group *Pbnm* at the Curie temperature $T_C = 1103$ K.³ It is classified as multiferroic due to the coexistence of ferroelectricity, ferroelasticity,⁴ and antiferromagnetism⁵ below the Néel temperature of 643 K. In principle, the solid state reaction between Bi₂O₃ and Fe₂O₃ is the simplest way to prepare BiFeO₃. However, in practice it has proven challenging to obtain single phase BiFeO₃ and avoid the formation of the secondary ternary oxides Bi₂₅FeO₃₉ and Bi₂Fe₄O₉. An early approach was solid state reaction with excess Bi₂O₃ followed by leaching with diluted nitric acid to wash away secondary ternary oxides and residual Bi₂O₃.⁶ More recently a successful method named “rapid liquid sintering” with stoichiometric ratio of binary oxide reactants has been reported; rapid heating to 1153 K followed by 7.5 min of soaking time and rapid cooling to ambient temperature.⁷ The difficulties of preparing single phase bismuth ferrite by solid state reaction have been attributed to the influence of small amounts of impurity phases,⁸ Bi₂₅FeO₃₉ and Bi₂Fe₄O₉ forming from the binary

oxides at low temperatures, and BiFeO₃ being unstable at high temperatures.⁹ A major advance in the understanding of solid state reaction synthesis of BiFeO₃ was presented by Valant et al.,⁸ which showed that the presence of impurities more soluble in Bi₂₅FeO₃₉ or Bi₂Fe₄O₉ than in BiFeO₃ reduced the stability of BiFeO₃. Here we investigate the influence of temperature on the thermodynamic stability of BiFeO₃ relative to the undesired ternary phases. BiFeO₃ is proposed to be metastable with respect to Bi₂Fe₄O₉ and Bi₂₅FeO₃₉ between 720 and 1040 K based on in situ high temperature X-ray diffraction (XRD) and ex situ XRD after isothermal heat treatment and recently reported thermodynamic data.¹⁰ These findings are discussed in relation to synthesis and the stability of BiFeO₃ and related Bi-based perovskites. We also address the stability of BiFeO₃ relative to its binary oxides and the effect of chemical substitution on A and B site.

Experimental Section

BiFeO₃ and BiFe_{0.7}Mn_{0.3}O₃ for in situ HTXRD studies was prepared by solid state reaction of Bi₂O₃ (Aldrich, >99.9%), Fe₂O₃ (Merck, >99%), and Mn₂O₃ (prepared by calcination of Mn(NO₃)₂·4H₂O Merck, >98.5% at 1073 K for 8 h). Dried starting materials were mixed by ball milling in ethanol for 24 h and fired once at 1098 K for 8 h with 400 K h⁻¹ heating and cooling rates. Starting materials for isothermal heat treatments were a ball milled and dried Bi₂O₃–Fe₂O₃ mixture and a phase pure BiFeO₃ powder prepared by a wet chemical route described elsewhere.¹¹ Fresh powder samples were used for each isothermal heat treatment.

HTXRD characterization of BiFeO₃ was performed on a θ - θ Bruker AXS D8 ADVANCE diffractometer with a high temperature stage (mri Physikalische Geäte GmbH), a VANTEC-1 detector, Cu K α radiation, and a secondary monochromator. For each temperature, the data collection time was 5.5 h over the range 20–120° 2 θ . BiFe_{0.7}Mn_{0.3}O₃ was characterized with a Siemens D5005 θ - θ

* To whom correspondence should be addressed. E-mail: tor.grande@material.ntnu.no.

- (1) Eerenstein, W.; Mathur, N. D.; Scott, J. F. *Nature* **2006**, *442*, 759–765.
- (2) Wang, J.; Neaton, J. B.; Zheng, H.; Nagarajan, V.; Ogale, S. B.; Liu, B.; Viehland, D.; Vaithyanathan, V.; Schlom, D. G.; Waghmare, U. V.; Spaldin, N. A.; Rabe, K. M.; Wuttig, M.; Ramesh, R. *Science* **2003**, *299*, 1719–1722.
- (3) Arnold, D. C.; Knight, K. S.; Morrison, F. D.; Lightfoot, P. (<http://arxiv.org/pdf/0811.1501>).
- (4) Kubel, F.; Schmid, H. *Acta Crystallogr.* **1990**, *B46*, 698–702.
- (5) Moreau, J. M.; Michel, C.; Gerson, R.; James, W. J. *J. Phys. Chem. Solids* **1971**, *32*, 1315–1320.
- (6) Achenbach, G. D.; James, W. J.; Gerson, R. *J. Am. Ceram. Soc.* **1967**, *50*, 437.
- (7) Wang, Y. P.; Zhou, L.; Zhang, M.F.; Chen, X. Y.; Liu, J. M.; Liu, Z. G. *Appl. Phys. Lett.* **2004**, *84*, 1731–1733.
- (8) Valant, M.; Axelsson, A.-K.; Alford, N. *Chem. Mater.* **2007**, *19*, 5431–5436.

(9) Morozov, M. I.; Lomanova, N. A.; Gusarov, V. V. *Russ. J. Gen. Chem.* **2003**, *73*, 1676–1680.

(10) Phapale, S.; Mishra, R.; Das, D. *J. Nucl. Mater.* **2008**, *373*, 137–141.

(11) Selbach, S. M.; Einarsrud, M.-A.; Tybell, T.; Grande, T. *J. Am. Ceram. Soc.* **2007**, *90*, 3430–3434.

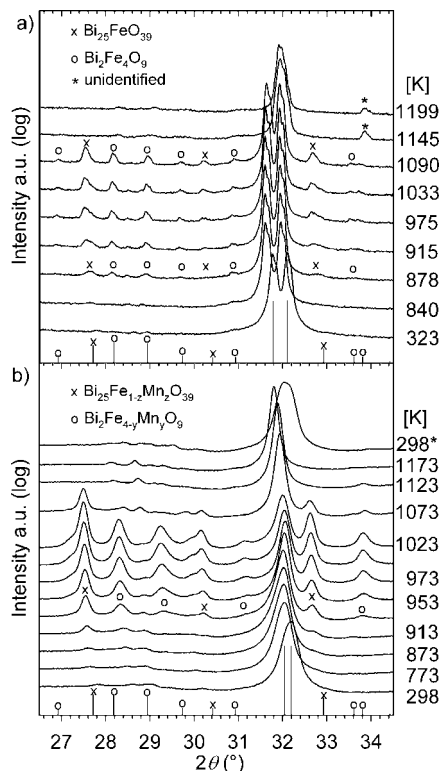


Figure 1. High temperature X-ray diffraction of (a) BiFeO_3 and (b) $\text{BiFe}_{0.7}\text{Mn}_{0.3}\text{O}_3$. Secondary ternary phases $\text{Bi}_{25}\text{FeO}_{39}$ (\times) (JCPDS 46–0416) and $\text{Bi}_2\text{Fe}_4\text{O}_9$ (\circ) (JCPDS 72-1832) form at the expense of the perovskite phase above 873 K but react back to the perovskite phase at higher temperatures. The diffractogram labeled 298* in (b) was recorded after cooling from 1173 to 298 K.

diffractometer with a high temperature camera (HTK 16, Anton Paar, GmbH) using $\text{Cu K}\alpha$ radiation and a primary monochromator. For each temperature, the data collection time was 5.1 h over the range 19 to $96^\circ 2\theta$. Prior to each subsequent scan the powder samples were held for 30 min at the temperature to establish thermal equilibrium. Pressed pellet samples covered with sacrificial powder were isothermally heat treated at 923 K (150 h), 1048 K (150 h), and 1123 K (8 h). Ex situ XRD of isothermally heat treated samples was done with the D8 ADVANCE diffractometer.

Results and Discussion

HTXRD of BiFeO_3 in Figure 1a demonstrates the formation of $\text{Bi}_{25}\text{FeO}_{39}$ (\times) and $\text{Bi}_2\text{Fe}_4\text{O}_9$ (\circ) at 878 K. The two main peaks of BiFeO_3 are shown as unlabeled bars at 31.78° and $32.10^\circ 2\theta$. The relative intensities of the Bragg reflections demonstrate the growth of $\text{Bi}_{25}\text{FeO}_{39}$ and $\text{Bi}_2\text{Fe}_4\text{O}_9$ at the expense of BiFeO_3 up to 1090 K. At higher temperatures the Bragg reflections of $\text{Bi}_{25}\text{FeO}_{39}$ and $\text{Bi}_2\text{Fe}_4\text{O}_9$ disappear, implying that these phases react back to the perovskite phase. The volatility of bismuth rich compounds cannot explain these observations since this would result in residual Fe_2O_3 or $\text{Bi}_2\text{Fe}_4\text{O}_9$. In contradiction with previous reports,⁹ we do not observe decomposition of BiFeO_3 between 1090 and 1199 K, even at long data collection times. Thus BiFeO_3 is a thermodynamically stable compound in the paraelectric state up to the peritectic decomposition temperature¹² of 1207 K. The same thermal evolution of the diffractograms is seen

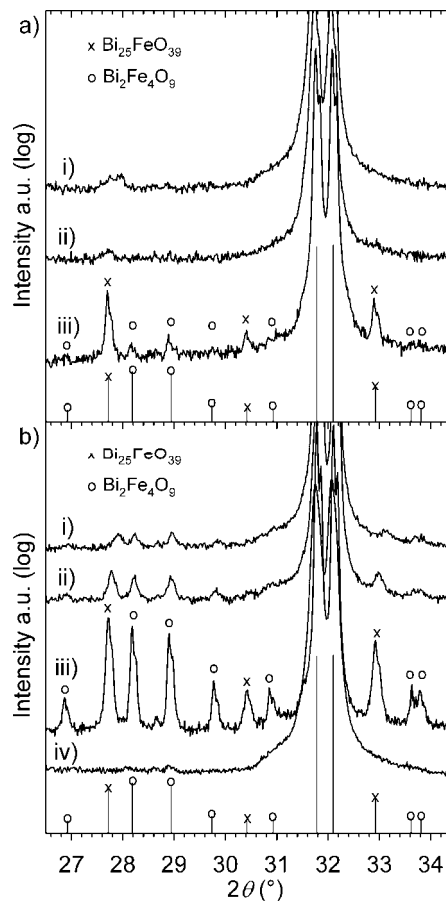
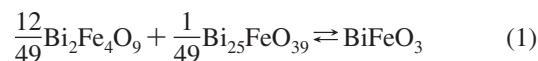


Figure 2. Ex situ X-ray diffraction of isothermally heat treated $\text{Bi}_2\text{O}_3\text{--Fe}_2\text{O}_3$ mixture (a) and initially phase pure BiFeO_3 (b). The labels i, ii, iii, and iv refer to 1123, 1048, 973, and 298 K (before heat treatment), respectively.

for $\text{BiFe}_{0.7}\text{Mn}_{0.3}\text{O}_3$, with nucleation of $\text{Bi}_2\text{Fe}_{4-y}\text{Mn}_y\text{O}_9$ and $\text{Bi}_{25}\text{Fe}_{1-z}\text{Mn}_z\text{O}_{39}$ around 873 K and subsequent growth up to 1023 K. At 1073 K the intensities of the secondary ternary oxides have decreased, as they react back to the perovskite phase.

Ex situ XRD of isothermally heat treated $\text{Bi}_2\text{O}_3\text{--Fe}_2\text{O}_3$ mixture and phase pure BiFeO_3 are shown in Figure 2. Substantial amounts of $\text{Bi}_{25}\text{FeO}_{39}$ and $\text{Bi}_2\text{Fe}_4\text{O}_9$ are evident after firing at 927 K, while minor amounts are present at 1048 and 1123 K. Larger amounts of mullite and sillenite phase are observed in the initially phase pure and fine-grained material from a wet chemical route than the initial $\text{Bi}_2\text{O}_3\text{--Fe}_2\text{O}_3$ mixture. From the annealing experiments of phase pure BiFeO_3 at 927 K it was shown that the amount of $\text{Bi}_{25}\text{FeO}_{39}$ and $\text{Bi}_2\text{Fe}_4\text{O}_9$ was growing with time in line with a recent report.¹³

The chemical reaction observed in the case of BiFeO_3 in Figures 1a and 2b is¹³



In the following, only the case on BiFeO_3 will be discussed, as the same principles also will apply to $\text{BiFe}_{0.7}\text{Mn}_{0.3}\text{O}_3$. In line with Gibbs' phase rule the three phases can coexist with zero degrees of freedom, as the

(12) Maître, A.; François, M.; Gachon, J. C. J. *Phase Equilib.* **2004**, *25*, 59–67.

(13) Carvalho, T. T.; Tavares, P. B. *Mater. Lett.* **2008**, *62*, 3984–3986.

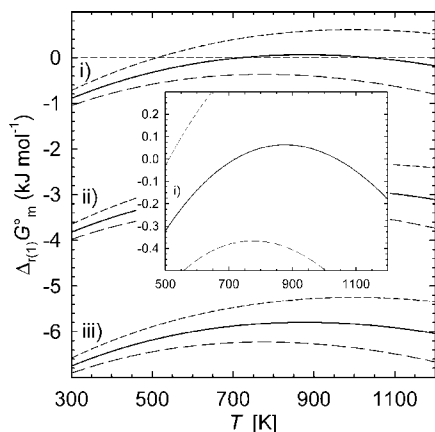


Figure 3. Gibbs energy (for one mol BiFeO₃) of reaction 1, $\Delta_{r(1)}G_m^\circ(T)$ with $\Delta_{r(1)}H_m^\circ(298.15) = -1980$ (i), -4910 (ii), and -7840 J mol⁻¹ (iii), respectively, and $\Delta_{r(1)}S_m^\circ(298.15) = -3.62$ (solid line), -4.2 (long dash), and -3.1 (short dash) J K⁻¹ mol⁻¹, respectively. Inset: $\Delta_{r(1)}G_m^\circ(T)$ with $\Delta_{r(1)}H_m^\circ(298.15) = -1980$ J mol⁻¹, implying that BiFeO₃ is metastable with respect to Bi₂Fe₄O₉ and Bi₂₅FeO₃₉ for 720 K < T < 1040 K as $\Delta_{r(1)}G_m^\circ(T) > 0$, in line with the XRD data in Figures 1 and 2.

number of components is two, since the oxidation state of Fe does not change, and the system can be described as the pseudobinary system Bi₂O₃–Fe₂O₃. Given that BiFeO₃ is stable above 1040 K, the molar Gibbs energy of reaction 1, $\Delta_{r(1)}G_m^\circ$, must change sign from positive to negative at 1040 K. According to $\Delta_{r(1)}G_m^\circ = \Delta_{r(1)}H_m^\circ - T\Delta_{r(1)}S_m^\circ$, both $\Delta_{r(1)}H_m^\circ$ and $\Delta_{r(1)}S_m^\circ$ must thus be positive. Solution calorimetry data from Phapale et al.¹⁰ give an enthalpy of reaction at ambient close to zero: $\Delta_{r(1)}H_m^\circ = -4.91 \pm 2.93$ kJ mol⁻¹; hence, reaction 1 is weakly exothermic at room temperature. $\Delta_{r(1)}G_m^\circ$ may change sign from positive to negative at 1040 K if both $\Delta_{r(1)}H_m^\circ$ and $\Delta_{r(1)}S_m^\circ$ also change signs from negative to positive at temperatures lower than 1040 K. To examine this scenario we apply the difference in molar heat capacity for reaction 1, $\Delta_{r(1)}C_{p,m}^\circ$, derived from $C_{p,m}^\circ$ reported¹⁰ for BiFeO₃, Bi₂Fe₄O₉, and Bi₂₅FeO₃₉ weighted according to the stoichiometry of reaction 1: $\Delta_{r(1)}C_{p,m}^\circ(T) = 2.74 + 1.96 \times 10^{-3}T - 9.4797 \times 10^4 T^{-2}$ J K⁻¹ mol⁻¹. At $T_{eq} \approx 1040$ K, $\Delta_{r(1)}G_m^\circ = 0$ and $\Delta_{r(1)}H_m^\circ(T_{eq}) = T_{eq}\Delta_{r(1)}S_m^\circ(T_{eq})$, where

$$\Delta_{r(1)}H_m^\circ(T_{eq}) = \Delta_{r(1)}H_m^\circ(298.15) + \int_{298.15}^{T_{eq}} \Delta_{r(1)}C_{p,m}^\circ dT \quad (2)$$

$$\Delta_{r(1)}S_m^\circ(T_{eq}) = \Delta_{r(1)}S_m^\circ(298.15) + \int_{298.15}^{T_{eq}} \frac{\Delta_{r(1)}C_{p,m}^\circ}{T} dT \quad (3)$$

$\Delta_{r(1)}S_m^\circ(298.15)$ is expected to be negative and close to zero, in line with the value of $\Delta_{r(1)}H_m^\circ(298.15)$, and the more open and disordered crystal structures of Bi₂Fe₄O₉ and Bi₂₅FeO₃₉ relative to BiFeO₃.^{14,15} Since $\Delta_{r(1)}C_{p,m}^\circ(T)$ is positive for $T > 300$ K, $\Delta_{r(1)}H_m^\circ(T)$ and $\Delta_{r(1)}S_m^\circ(T)$ will increase with temperature. $\Delta_{r(1)}G_m^\circ(T) = \Delta_{r(1)}H_m^\circ(T) - T\Delta_{r(1)}S_m^\circ(T)$ with $\Delta_{r(1)}H_m^\circ(298.15) = -4.91 \pm 2.93$ kJ mol⁻¹ is plotted in Figure 3, demonstrating the small difference in Gibbs energy of

reaction 1. $\Delta_{r(1)}G_m^\circ(T)$ is sensitive to the value of $\Delta_{r(1)}S_m^\circ(298.15)$, and as the inset of Figure 3 illustrates, with a value of -3.62 J K⁻¹ mol⁻¹ (solid line) $\Delta_{r(1)}G_m^\circ(T)$ evolves in concordance with the XRD data in Figures 1 and 2. $\Delta_{r(1)}G_m^\circ(T) > 0$ for approximately 720 K < T < 1040 K with $\Delta_{r(1)}H_m^\circ(298.15) = -1.98$ kJ mol⁻¹ and $\Delta_{r(1)}S_m^\circ(298.15) = -3.62$ J K⁻¹ mol⁻¹. In this temperature interval Bi₂Fe₄O₉ and Bi₂₅FeO₃₉ are weakly more stable (thermodynamically) than BiFeO₃. Observation of the partial decomposition in this temperature interval was only possible due the long HTXRD data collection times, owing to the small thermodynamic driving force and the low ionic mobility in the lower end of the temperature interval in question. The apparent contradiction that BiFeO₃ is seemingly metastable up to 1090 K in the HTXRD data compared to 1040 K in the ex situ XRD data follows from the small thermodynamic driving force for reaction 1 in this temperature region; thus, the reaction back to perovskite is slow. Influence of impurities as suggested by Valant et al.⁸ may also effect the observation as discussed further below.

BiFeO₃ is the energetically stable ternary compound at temperatures higher than 1040 K, but $\Delta_{r(1)}G_m^\circ(T)$ is close to zero. The XRD data in Figures 1 and 2 and the thermodynamic analysis in Figure 3 explains why firing a Bi₂O₃–Fe₂O₃ precursor at lower temperatures than 1040 K yields substantial amounts of Bi₂Fe₄O₉ and Bi₂₅FeO₃₉.^{7,16,17} In terms of obtaining single phase perovskite during solid state reaction synthesis, rapid heating of a Bi₂O₃–Fe₂O₃ precursor prevents initial formation of Bi₂Fe₄O₉ and Bi₂₅FeO₃₉, and fast cooling prevents the decomposition of BiFeO₃ shown in Figure 1. In addition the importance of pure precursors, small reactant powder particles, and precursor homogeneity has been pointed out earlier.^{8,11,18}

The influence of impurities on reaction 1 needs particular attention. It might be tempting to argue that the addition of several new chemical components (impurities) may lead to coexistence between the three pure phases BiFeO₃, Bi₂Fe₄O₉, and Bi₂₅FeO₃₉ (in terms of the Gibbs phase rule the number of independent components does increase). However, the coexistence of the pure phases is only possible when the Gibbs energy of reaction (1) is equal to zero (which only occurs at two specific temperatures, see Figure 3). On the other hand, if the solubility of the impurities is larger in Bi₂Fe₄O₉ or Bi₂₅FeO₃₉ than in BiFeO₃ the Gibbs energy of reaction 1 will be influenced and thereby effect the stability of BiFeO₃ relative to the Bi₂Fe₄O₉ and Bi₂₅FeO₃₉ solid solutions. Tentative phase diagrams provided by Valant et al.⁸ discuss this in detail (narrow three phase region consisting of BiFeO₃ in equilibrium with Bi₂₅Fe_{1-x}A_xO₃₉ and Bi₂Fe_{1-x}A_xO₉ where AO_y is the impurity oxide). A higher solubility of impurities in Bi₂Fe₄O₉ and/or Bi₂₅FeO₃₉ as discussed by Valant et al.⁸ will cause a thermodynamic destabilization of BiFeO₃ resulting in a shift upward in the Gibbs energy curve for reaction (1) shown in Figure 3. The effect of the impurities is to increase the temperature interval where Bi₂Fe₄O₉ and Bi₂₅FeO₃₉ are stable (destabilizing

(14) MacKenzie, K. J. D.; Dougherty, T.; Barrel, J. J. *Eur. Ceram. Soc.* **2008**, *28*, 499–504.

(15) Craig, D. C.; Stephenson, N. C. *J. Solid. State Chem.* **1975**, *15*, 1–8.

(16) Wang, Y. P.; Yuan, G. L.; Chen, X. Y.; Liu, J.-M.; Liu, Z. G. *J. Phys. D: Appl. Phys.* **2006**, *39*, 2019–2023.

(17) Nalwa, K. S.; Garg, A.; Upadhyaya, A. *Mater. Lett.* **2008**, *62*, 878–881.

(18) Yuan, G. L.; Or, S. W.; Wang, Y. P.; Liu, Z. G.; Liu, J. M. *Solid State Commun.* **2006**, *138*, 76–81.

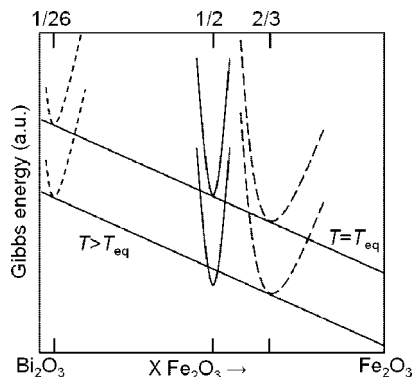


Figure 4. Schematic illustration of the Gibbs energy (a.u.) of BiFeO_3 (solid), $\text{Bi}_{25}\text{FeO}_{39}$ (short dash), and $\text{Bi}_2\text{Fe}_4\text{O}_9$ (long dash) as a function of nominal composition. At $T_{\text{eq}} = 1040$ K the tangent shows that the three phases are in equilibrium in line with Gibbs' phase rule. At $T > 1040$ K BiFeO_3 has lower Gibbs energy than $\text{Bi}_{25}\text{FeO}_{39}$ and $\text{Bi}_2\text{Fe}_4\text{O}_9$ which are in equilibrium, as their common tangent line lies higher in Gibbs energy than the Gibbs energy curve of BiFeO_3 .

BiFeO_3 in accordance with Valant et al.⁸). To summarize, the strong influence of impurities is caused by the small Gibbs energy difference between the reactants and the products in reaction 1. Impurities will therefore have a strong effect on the phase equilibrium and results in poor reproducibility if the impurity level, for example, alumina or silica from crucibles and so forth, is not well-controlled.

The influence of temperature and chemical homogeneity is illustrated schematically in Figure 4. The three ternary oxides are in equilibrium according to Gibbs' phase rule when $\Delta_{r,(1)}G_m^\circ(T_{\text{eq}}) = 0$, where the Gibbs energy curve of BiFeO_3 has a common tangent with the Gibbs energy curves of $\text{Bi}_2\text{Fe}_4\text{O}_9$ and $\text{Bi}_{25}\text{FeO}_{39}$. For $T > T_{\text{eq}}$ the Gibbs energy curve of BiFeO_3 is lower than the $\text{Bi}_2\text{Fe}_4\text{O}_9$ – $\text{Bi}_{25}\text{FeO}_{39}$ tangent line and BiFeO_3 is the stable compound. Deviation from 1:1 Bi_2O_3 : Fe_2O_3 stoichiometry will result in equilibrium between BiFeO_3 and one of the secondary ternary oxides, e.g. BiFeO_3 and $\text{Bi}_2\text{Fe}_4\text{O}_9$ due to evaporation of bismuth oxides. Moreover, the influence of pressure on reaction 1 is self-evident from the crystal structure of perovskite being close-packed compared to the mullite and sillenite structures of $\text{Bi}_2\text{Fe}_4\text{O}_9$ and $\text{Bi}_{25}\text{FeO}_{39}$, respectively.^{14,15} The volume change of reaction 1 is hence large and negative, $\Delta_{r,(1)}V_m = -5.14 \text{ cm}^3 \text{ mol}^{-1}$. The perovskite phase is thus favored by pressure and possibly compressive strain in thin films relative to the sillenite and mullite phase, and the $\Delta_{r,(1)}G_m^\circ(T)$ curves in Figure 3 will be shifted toward more negative values with increasing pressure.

We now address the thermodynamic stability of BiFeO_3 with respect to the end members Bi_2O_3 and Fe_2O_3 . The formation reaction from the binary oxides is



On the basis of solution calorimetry data,¹⁰ the enthalpy of reaction 4, the enthalpy of formation from oxides, $\Delta_{f,\text{ox}}H_m^\circ$, is $-70.75 \pm 3.40 \text{ kJ mol}^{-1}$ at 298.15 K. Yokokawa et al.¹⁹ first pointed out the relation between

(19) Yokokawa, H.; Kawada, T.; Dokiya, M. *J. Am. Ceram. Soc.* **1989**, *72*, 152–153.

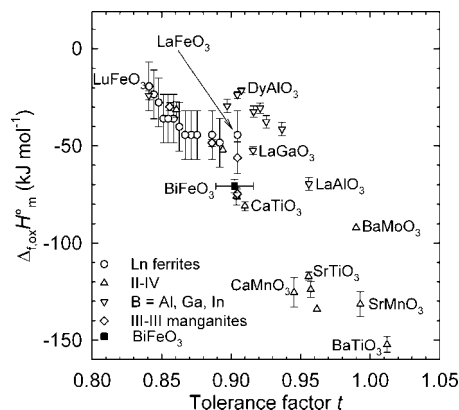


Figure 5. Standard enthalpies of formation for perovskites from binary oxides plotted as a function of the Goldschmidt tolerance factor. For direct comparison, all tolerance factors were calculated for nine-coordinated A cations. Thermodynamic data were adopted from refs 22–28.

$\Delta H_{f,\text{ox}}^\circ$ for perovskites and the Goldschmidt tolerance factor²⁰ $t = 2^{-1/2}(r_A + r_O)/(r_B + r_O)$, where r_A , r_B , and r_O are the ionic radii²¹ of the A cation, the B cation, and O^{2-} , respectively. BiFeO_3 follows this trend, as shown in Figure 5. For direct comparison, a coordination number (CN) of 9 was used for all A cations, as the radii of 12 coordinated cations are not available for many lanthanides and Bi^{3+} . The ionic radii of a $6s^2$ lone pair cation like Bi^{3+} is not straightforward and depends on the stereochemical activity of the lone pair.²¹ Hence, an uncertainty in terms of t is included in Figure 5, spanning from the values obtained for CN = 8 for Bi^{3+} to that for CN = 9 for the fairly equally sized cation La^{3+} .

Figure 5 suggests that isovalent substitution with a larger cation on the A site or a smaller cation on the B site would increase the stability of BiFeO_3 with respect to the binary oxides and possibly also with respect to the $\text{Bi}_2\text{Fe}_4\text{O}_9$ mullite and $\text{Bi}_{25}\text{FeO}_{39}$ sillenite phase. Substitution of a more acidic cation on the B site or a more basic cation on the A site is also expected to stabilize the perovskite phase.²⁸ La^{3+} is about the same size as Bi^{3+} , and although the space group changes with high substitution levels, perovskite phase is obtained with up to 40% La^{3+} .²⁹ Nd^{3+} , Sm^{3+} , and Gd^{3+} are smaller than Bi^{3+} , but more basic cations, and solid solutions prepared at ambient pressure have been reported up to 15–20% substitution.^{30–32} Mn^{3+} is the only cation reported to substitute Fe^{3+} by substantial

(20) Goldschmidt, V. M. *Naturwissenschaften* **1926**, *14*, 477.

(21) Shannon, R. D. *Acta Crystallogr.* **1976**, *A32*, 751–767.

(22) Morss, L. R. *J. Less-Common Met.* **1983**, *93*, 301–321.

(23) Kanke, Y.; Navrotsky, A. *J. Solid State Chem.* **1998**, *141*, 424–436.

(24) Laberty, C.; Navrotsky, A.; Rao, C. N. R.; Alphonse, P. *J. Solid State Chem.* **1999**, *145*, 77–87.

(25) Rørmark, L.; Stølen, S.; Wiik, K.; Grande, T. *J. Solid State Chem.* **2002**, *163*, 186–193.

(26) Takayama-Muromachi, E.; Navrotsky, A. *J. Solid State Chem.* **1988**, *72*, 244–256.

(27) Cheng, J. H.; Navrotsky, A. *J. Mater. Res.* **2003**, *18*, 2501–2508.

(28) Xu, H. W.; Navrotsky, A.; Su, Y. L.; Balmer, M. L. *Chem. Mater.* **2005**, *17*, 1880–1886.

(29) Zhang, S.-T.; Pang, L.-H.; Zhang, Y.; Lu, M.-H.; Chen, Y.-F. *J. Appl. Phys.* **2006**, *100*, 114108.

(30) Yuan, G. L.; Or, S. W. *Appl. Phys. Lett.* **2006**, *88*, 062905.

(31) Yan, Y. Z.; Wang, K. F.; Qu, J. F.; Wang, Y.; Song, Z. T.; Feng, S. L. *Appl. Phys. Lett.* **2007**, *91*, 082906.

(32) Chang, F. G.; Song, G. L.; Fang, K.; Qin, P.; Zeng, Q. *J. J. Rare Earths* **2006**, *24*, 273–276.

amounts (30%) with solid state reaction synthesis at ambient pressure.³³ Al³⁺, Ga³⁺, and Cr³⁺ cannot be substituted by 5–20% at ambient pressure, resulting only in mullite and sillenite phases (results not reported here), while BiAlO₃, BiGaO₃, and BiCrO₃ can be prepared by high pressure synthesis.^{34–36} Even though Al³⁺, Ga³⁺, and Cr³⁺ are smaller than high spin Fe³⁺, and the effective tolerance factors would increase with substitution, equilibrium 1 is shifted completely toward the left with substitution of Al³⁺, Ga³⁺, or Cr³⁺, implying no solid solubility in BiFeO₃ at ambient pressure. The presence of only 0.1 and 0.5% Al₂O₃ in the system thus yields a large amount of sillenite and mullite phases, as reported

by Valant et al.⁸ This is in accordance with our analysis of the effect of impurities presented above. The large negative value of $\Delta_{r(1)}V_m$ explains why reaction 1 is shifted toward the right with high pressure, allowing the formation of BiAlO₃, BiGaO₃, and BiCrO₃.

Conclusion

In summary, BiFeO₃ is shown to be metastable with respect to Bi₂Fe₄O₉ (mullite phase) and Bi₂₅FeO₃₉ (sillenite phase) for 720 < *T* < 1040 K. The observation can be explained by thermodynamic considerations. The thermodynamic stability of BiFeO₃-based solid solution perovskites relative to mullite and sillenite phases can be rationalized in terms of tolerance factor, acid–base relations, chemical substitution, and pressure.

Acknowledgment. This work was supported by the Norwegian University of Science and Technology and the Research Council of Norway (NANOMAT, Grants 158518/431, 140553/I30, and 162874/V00).

CM802607P

-
- (33) Yang, C.-H.; Koo, T. Y.; Jeong, Y. H. *Solid State Commun.* **2005**, *134*, 299–301.
- (34) Belik, A. A.; Wuernisha, T.; Kamiyama, T.; Mori, K.; Maie, M.; Nagai, T.; Matsui, Y.; Takayama-Muromachi, E. *Chem. Mater.* **2006**, *18*, 133–139.
- (35) Niikata, S.; Azuma, M.; Takano, M.; Nishibori, E.; Takata, M.; Sakata, M. *Solid State Ionics* **2004**, *172*, 557–559.
- (36) Belik, A. A.; Iikubo, S.; Kodoma, K.; Igawa, N.; Shamoto, S.; Takayama-Muromachi, E. *Chem. Mater.* **2008**, *20*, 3765–3769.